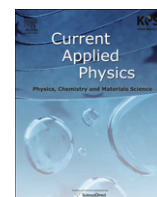




Contents lists available at ScienceDirect

Current Applied Physics

journal homepage: www.elsevier.com/locate/cap

Poling dependence and stability of piezoelectric properties of $\text{Ba}(\text{Zr}_{0.2}\text{Ti}_{0.8})\text{O}_3-(\text{Ba}_{0.7}\text{Ca}_{0.3})\text{TiO}_3$ ceramics with huge piezoelectric coefficients

Shi Su^a, Ruzhong Zuo^{a,*}, Shengbo Lu^b, Zhengkui Xu^b, Xiaohui Wang^c, Longtu Li^c

^a Institute of Electro Ceramics & Devices, School of Materials Science and Engineering, Hefei University of Technology, Hefei 230009, China

^b Department of Physics and Materials Science, City University of Hong Kong, Hong Kong, China

^c State Key Lab of New Ceramics and Fine Processing, Department of Materials Science and Engineering, Tsinghua University, Beijing 100084, China

ARTICLE INFO

Article history:

Received 22 June 2010

Received in revised form

18 January 2011

Accepted 25 January 2011

Available online 4 February 2011

Keywords:

Lead-free

Dielectric

Piezoelectric

Aging

ABSTRACT

Poling dependence and stability of piezoelectric properties of lead-free $0.5\text{Ba}(\text{Zr}_{0.2}\text{Ti}_{0.8})\text{O}_3-0.5(\text{Ba}_{0.7}\text{Ca}_{0.3})\text{TiO}_3$ ceramics were investigated. The experimental results indicated that the poling condition has an obvious effect on the piezoelectric properties due to the existence of a phase transition near room temperature. The best piezoelectric coefficient d_{33} and planar electromechanical coupling factor k_p could reach 630 pC/N and 56%, respectively as the poling conditions were optimized. However, these properties exhibit strong temperature and time dependences, owing to a rather low depolarization temperature (below 80–90 °C) and extremely high aging rate (30% and 25% loss for d_{33} and k_p , respectively, 10^4 min after poling).

© 2011 Elsevier B.V. All rights reserved.

1. Introduction

$\text{Pb}(\text{Zr},\text{Ti})\text{O}_3$ based piezoelectric ceramics have been commercially used for more than half a century based on their excellent piezoelectric and electromechanical properties. Increasing concerns about Pb pollution have brought much attention to lead-free piezoelectric compositions in last few years [1,2]. Several typical lead-free systems have been highlighted such as BaTiO_3 (BT) based systems, $(\text{Bi}_{0.5}\text{Na}_{0.5})\text{TiO}_3$ based systems and $(\text{Na}_{0.5}\text{K}_{0.5})\text{NbO}_3$ (NKN) based systems. The piezoelectric properties of these systems have been significantly enhanced through different processing routes, some of which get close to those of PZT ceramics. However, none of these systems are perfect in electrical properties. By comparison, modified BT based compositions seem to own a great potential considering their extremely large piezoelectric coefficient d_{33} reported recently [3–8]. BT ceramics prepared by two-step sintering were reported to have a large piezoelectric coefficient ($d_{33} > 460$ pC/N) [4]. Moreover, the electrical properties of pure BT ceramics have been also significantly enhanced by adding a small amount of BaZrO_3 (BZ) [9]. Particularly,

well-designed lead-free ceramics of BZ-BT- CaTiO_3 solid solutions have been recently reported by Liu and Ren [8], which exhibit extremely large piezoelectric activities.

However, it is generally believed that BT based piezoelectric materials mainly suffer from low Curie temperatures (T_C), which may restrict their potential applications to a large extent. Furthermore, their temperature and time stabilities also need to be explored in terms of possible device applications. The aging behavior is usually attributed to a gradual stabilization of ferroelectric domains by some defects [10–13], which may strongly affect the reliability of devices. Moreover, a poling is usually necessary before ferroelectric ceramics can exhibit piezoelectric effects, which is actually a process of domain reorientation and domain wall movement driven by an external electric field. Therefore, the optimization of poling conditions, such as temperature, electric field and poling time, can produce the best piezoelectric performances since all three parameters will influence the domain reorientation and wall movement [14,15].

This study was focused on the poling dependence and stability of piezoelectric properties of $0.5\text{Ba}(\text{Zr}_{0.2}\text{Ti}_{0.8})\text{O}_3-0.5(\text{Ba}_{0.7}\text{Ca}_{0.3})\text{TiO}_3$ (BZT-BCT) ceramics with huge piezoelectric activities. This composition was reported to lie close to a tricritical point of rhombohedral, tetragonal and cubic phases [8]. The relationship between the property and phase structure was also discussed.

* Corresponding author. Tel./fax: +86 551 2905285.
E-mail address: piezolab@hfut.edu.cn (R. Zuo).

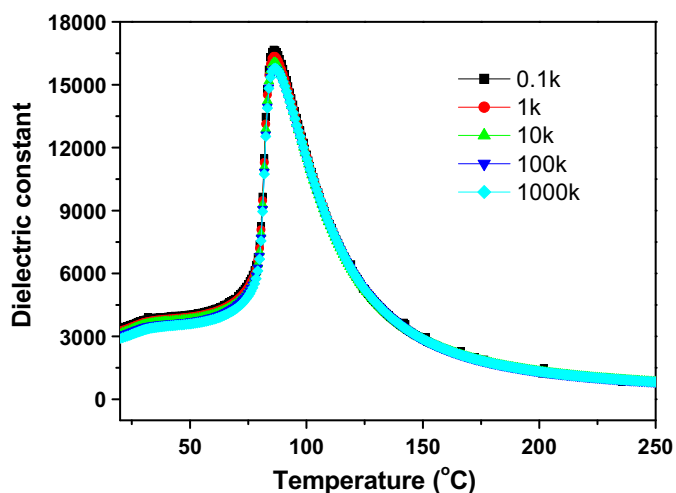


Fig. 1. The dielectric constant of BZT-BCT ceramics as a function of measuring temperature and frequency.

2. Experimental procedures

High-purity raw chemicals, BaCO_3 ($\geq 99.0\%$), CaCO_3 ($\geq 99.0\%$), TiO_2 ($\geq 99.0\%$) and ZrO_2 ($\geq 99.0\%$) were used in this study. The BZT-BCT powder was prepared through the solid state reaction method. The powders were weighed according to the chemical formula and then mixed for 12 h in a planetary ball mill using alcohol as the media. After calcination at $1350\text{ }^\circ\text{C}$ for 4 h, the resultant powder was milled for 24 h and then pressed into disk specimens with a diameter of $\sim 10\text{ mm}$ and a thickness of $\sim 1\text{ mm}$ only by uniaxial pressing with a pressure of 150 MPa. During compaction, no binder was used. Sintering was carried out in the temperature range of $1450\text{ }^\circ\text{C}$ – $1500\text{ }^\circ\text{C}$ for 3 h with a heating rate of $5\text{ }^\circ\text{C}/\text{min}$.

For electrical measurements, silver paste was coated on major surfaces and then fired at $550\text{ }^\circ\text{C}$ for 30 min. The electric poling was performed in the range of $20\text{ }^\circ\text{C}$ – $80\text{ }^\circ\text{C}$ in a silicone oil bath by applying a dc field of $1.5E_c$ to $3E_c$ for 20 min and the electric field was maintained during cooling. The dielectric constant of unpoled samples was measured as a function of temperature by an LCR meter (Agilent E4980A, Santa Clara, CA, USA) equipped with a temperature box. Polarization versus electric field (P – E) hysteresis loops were measured at different temperatures using a ferroelectric measuring system (Precision LC, Radiant Technologies, Inc. Albuquerque, NM, USA). The piezoelectric constant d_{33} was measured by a Belincourt-meter (YE2730A, Sinocera, Yangzhou, China). The planar electromechanical coupling factor k_p was determined by a resonance–antiresonance method with an impedance analyzer (Impedance Analyzer, PV70A, Beijing, China). Two groups of poled samples were placed under dry and wet conditions for days after which the piezoelectric properties were measured again to study the time stability of piezoelectric property. Some poled samples were annealed at different temperatures and their piezoelectric properties at room temperature were remeasured as the evaluation of thermal stability. Domain structure of BZT-BCT samples was examined with a transmission electron microscope (TEM, JEM-2010F). TEM specimens were prepared by mechanically polishing samples to $\sim 10\text{ }\mu\text{m}$ that were transferred onto a copper grid and then by ion milling to perforation.

3. Results and discussion

The dielectric constant of unpoled BZT-BCT ceramics as a function of temperature and frequency is shown in Fig. 1. It can be seen that the composition owns a polymorphic phase transition (PPT) between rhombohedral and tetragonal phases near room temperature and a Curie temperature of $\sim 90\text{ }^\circ\text{C}$. Moreover, the dielectric constant shows only slight frequency dependence. Its value at room temperature reaches as high as 3000. These results are consistent

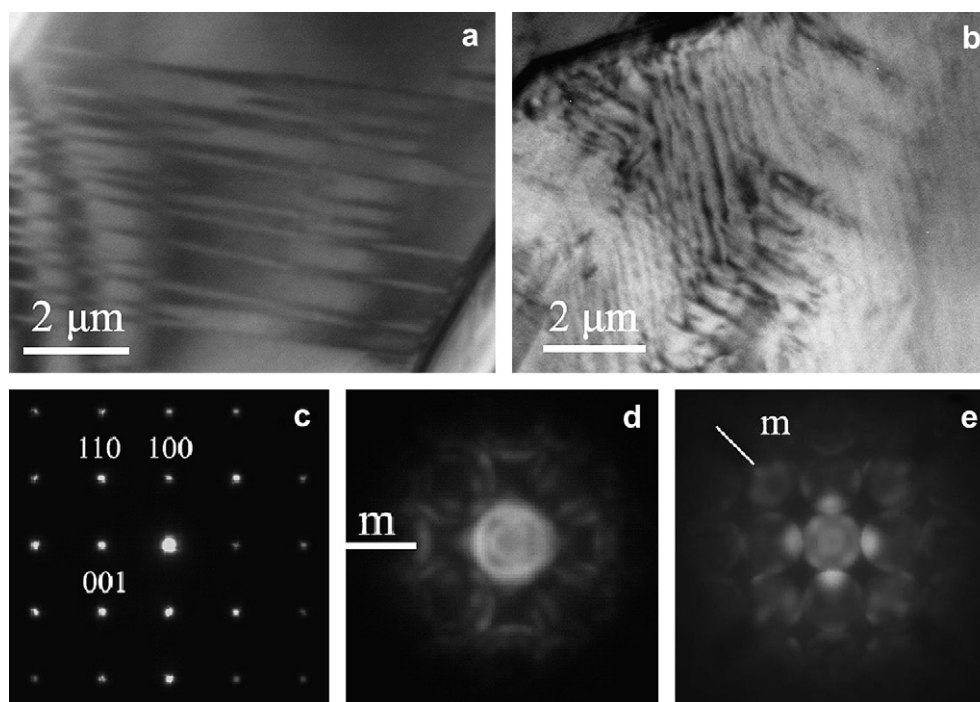


Fig. 2. (a) and (b) Bright-field images of two grains in BZT-BCT ceramics, (c) $\langle 100 \rangle$ SAED pattern obtained from the two grains, and (d) and (e) corresponding two CBED $\langle 100 \rangle$ patterns, respectively.

well with those previously reported [8]. The PPT near room temperature leads to the coexistence of rhombohedral and tetragonal phases, which is similar to that in NKN based systems [2]. Preliminary results of TEM study indicated the coexistence of tetragonal and rhombohedral phases in BZT-BCT ceramics, as illustrated in Fig. 2. Fig. 2(a) and (b) is two bright-field images of domains recorded from two different grains and a similar $\langle 100 \rangle$ SAED pattern was obtained from these two grains, as shown in Fig. 2(c). Fig. 2(d) and (e) is the corresponding two CBED $\langle 100 \rangle$ patterns obtained from the grains in (a) and (b), respectively, and a mirror plane can be appreciated along $\langle 001 \rangle$ direction in (d) and along $\langle 110 \rangle$ direction in (e), indicating that the grain in (a) has a tetragonal structure and the grain in (b) has a rhombohedral structure. However, the dominant phase in BZT-BCT is rhombohedral by judging different domain morphologies observed when the grains were tilted to certain directions. It was thought that the phase coexistence may induce extremely high piezoelectric activity. However, a PPT close to room temperature and a low T_c value could probably induce thermal stability issues of piezoelectric properties.

Fig. 3 indicates P – E hysteresis loops of unpoled BZT-BCT ceramics at different temperatures. It is evident that the ceramics are typically soft, with a very low coercive field E_c of 0.27 kV/mm and a relatively high remnant polarization P_r of $\sim 13 \mu\text{C}/\text{cm}^2$. Hysteresis loops become slimmer and slimmer with increasing temperature, accompanied by a fast drop of P_r values. The loop looks almost closed as the temperature is over 80°C , indicating that ferroelectric domains disappear. This result is in good agreement with the measurement of the dielectric constant versus temperature as shown in Fig. 1.

The piezoelectric properties of BZT-BCT ceramics poled under different conditions are shown in Fig. 4. The BZT-BCT ceramics have extremely high piezoelectric responses of $d_{33} = 630 \text{ pC/N}$ and $k_p = 56\%$, compared to other lead-free ceramics. In addition, these piezoelectric properties exhibit obvious dependence on the poling condition. The low poling electric field makes the polarization switching inadequate. However, excessive poling electric field tends to over-pole the samples which lead to physical flaws and eventually to the dielectric breakdown of the samples [15]. The optimum poling electric field for BZT-BCT ceramics is about two times that of E_c , as shown in Fig. 4(a). Moreover, the maximum piezoelectric properties appear in the temperature range of 30°C – 40°C in which

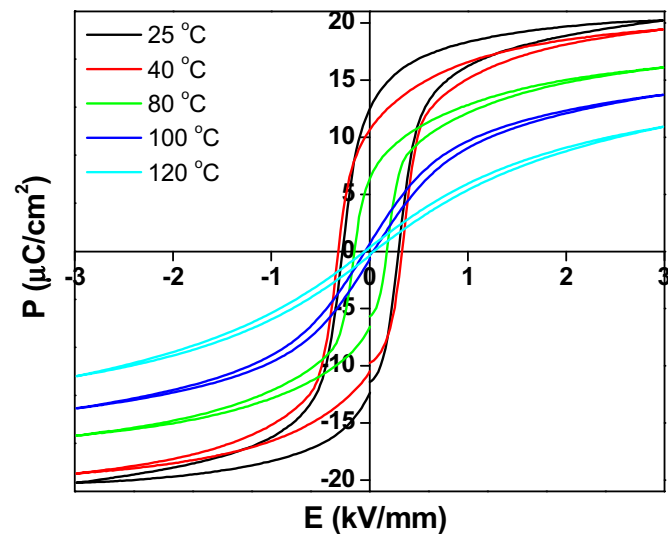


Fig. 3. P – E hysteresis loops of BZT-BCT ceramics measured at different temperatures as indicated.

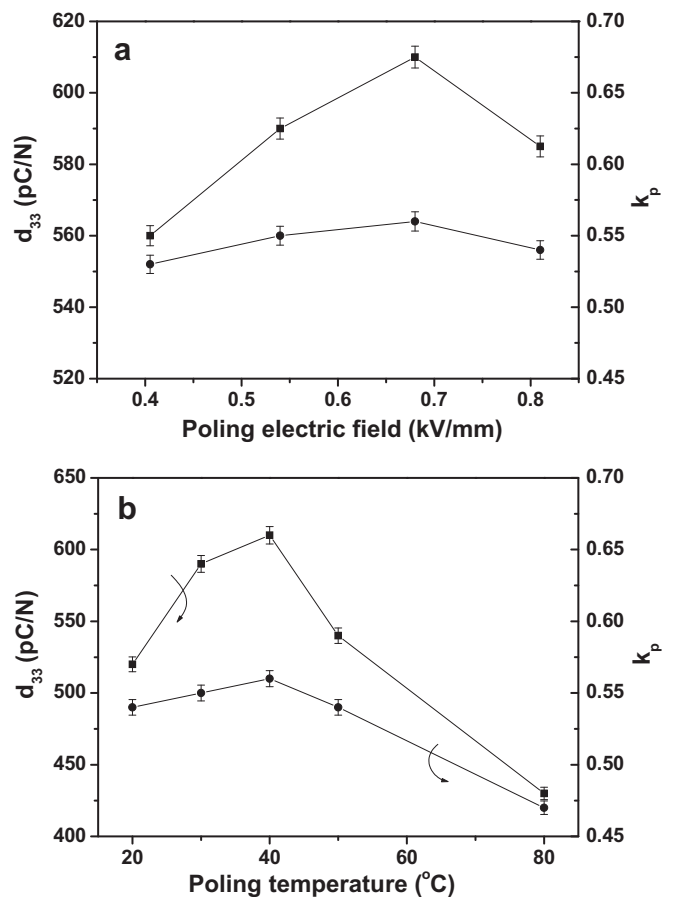


Fig. 4. The piezoelectric properties of BZT-BCT ceramics as a function of the poling (a) electric field (the poling temperature is 40°C) and (b) temperature (the poling electric field is $2.5E_c$).

both rhombohedral and tetragonal phases coexist [8]. The piezoelectric properties of poled BZT-BCT ceramics were measured after annealing samples at different temperatures, as shown in Fig. 5. It can be seen that both d_{33} and k_p values exhibit a fast drop with increasing the annealing temperatures ($\sim 20\%$ loss till 80°C) and then completely disappear owing to the ferroelectric-paraelectric phase transition at $\sim 90^\circ\text{C}$. Such a low Curie temperature greatly limits the permitted working temperature range, as also reflected in Figs. 1 and 3. Moreover, the thermal instability of piezoelectric

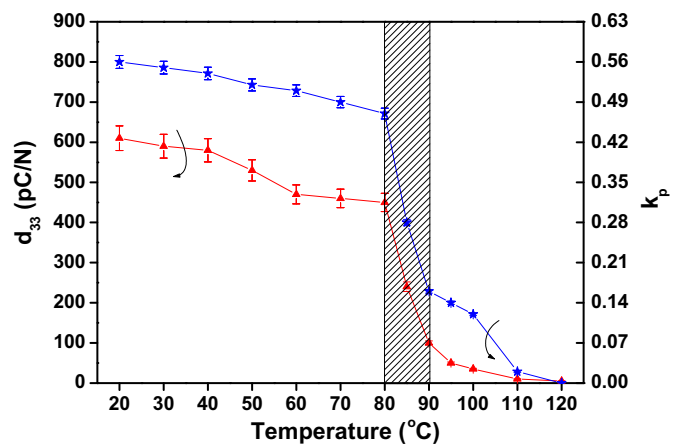


Fig. 5. Thermal stability of the piezoelectric properties of poled BZT-BCT ceramics.

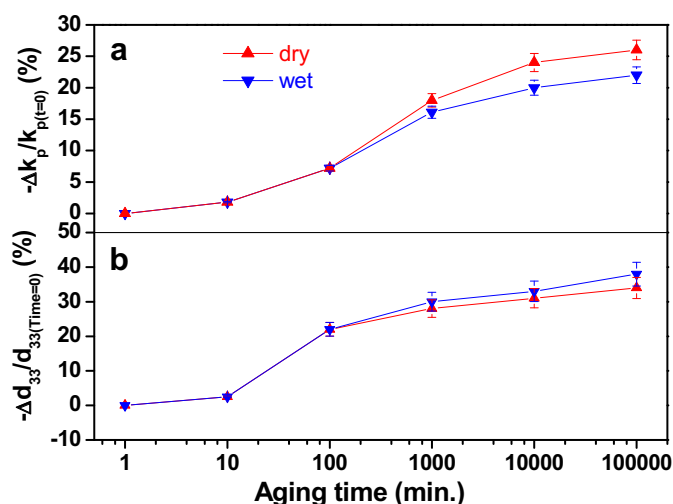


Fig. 6. The relative variation of (a) k_p and (b) d_{33} as a function of the aging time (room temperature).

properties induced by a rhombohedral–tetragonal PPT may not be ignored, which is quite similar to that in NKN based lead-free piezoelectric compositions [16–19]. The argument that the above-mentioned phase transition belongs to the morphotropism in nature is thus doubted [8]. On the contrary, the formation of phase coexistence in BZT–BCT ceramics actually originated from the relative movement between rhombohedral–orthorhombic and orthorhombic–tetragonal PPT temperatures in BT, which leads to the atrophy of orthorhombic zone. The substitution of Zr^{4+} for Ti^{4+} was known to increase these two temperatures however the substitution of Ca^{2+} for Ba^{2+} tends to decrease them [1,8,9,20–25]. Therefore, the coexistence of rhombohedral (R), orthorhombic (O) and tetragonal (T) phases in BZT–BCT samples could be possible in a certain temperature range, which is intrinsically the polymorphism (the R–O transition and O–T transition are included).

Fig. 6 shows the relative variation of piezoelectric properties as a function of aging time of poled BZT–BCT ceramics that were placed under wet and dry conditions at room temperature. Little effect of humidity on aging behavior of piezoelectric properties of BZT–BCT ceramics was observed, indicating that this material system exhibits good resistance to the humidity. However, this is a serious issue for NKN based compositions [26]. On the other hand, it can be seen that the piezoelectric properties of the samples degrade extremely fast within 10^4 min after poling (d_{33} and k_p were lost by $\sim 30\%$ and $\sim 25\%$, respectively) and gradually become stable. In general, large internal stress induced by 90° domain wall motion and reorientation of ferroelectric domains tends to force part of oriented domains to switch back [27,28], which could be more significant in a tetragonal phase where 90° domain is dominant, compared to a rhombohedral phase. The reason is that the switching of 90° domain is accompanied by a certain strain. As a result, the piezoelectric properties will degrade with time after the poling electric field was removed. Therefore, the aging behavior could be better in a rhombohedral phase than in a tetragonal phase [29]. However, the unusual aging behavior in this material could be also ascribed to the multi-phase coexistence at the proximity of tricritical points where domain orientation becomes easier during electric poling, but domains could switch back more easily as well after electric field is released based on the same reason.

The coexistence of multi-phases makes the energy barrier smaller during polarization switching.

4. Conclusions

The poling dependence and stability of piezoelectric properties of BZT–BCT ceramics were investigated. The optimal poling conditions are $2.5E_c$ and $40^\circ C$ for poling field and temperature, respectively, under which huge d_{33} and k_p values of 630 pC/N and 56% can be obtained. However, these properties exhibited significant temperature and time dependences, which were discussed in correlation with the nature of phase transition and phase coexistence. The coexistence of multi-phases close to tricritical points might make oriented domains relatively easily switch back such that a fast aging behavior occurs just after poling electric field is removed.

Acknowledgements

This work was financially supported by a project of Natural Science Foundation of Anhui Province (090414179), a Program for New Century Excellent Talents in University, State Education Ministry (NCET-08-0766) and a 973 Program (No. 2009CB623301), and also partially supported by a grant from the Research Grants Council of the Hong Kong Special Administrative Region, China (No. 9041211).

References

- [1] B. Jaffe, W.R. Cook, H. Jaffe, *Piezoelectric Ceramics*. Academic Press, New York, 1971.
- [2] Y. Saito, H. Takao, T. Tani, T. Nonoyama, K. Takatori, T. Homma, T. Nagaya, M. Nakamura, *Nature* 432 (2004) 84.
- [3] H.Y. Tian, Y. Wang, J. Miao, H.L.W. Chan, C.L. Choy, *J. Alloys Compd.* 431 (2007) 197.
- [4] T. Karaki, K. Yan, M. Adachi, *Jpn. J. Appl. Phys.* 46 (2007) 7035.
- [5] D.S. Fu, M. Itoh, S.Y. Koshihara, *Appl. Phys. Lett.* 93 (2008) 012904.
- [6] H. Takahashi, Y. Numamoto, J. Tani, S. Tsurekawa, *Jpn. J. Appl. Phys.* 47 (2008) 8468.
- [7] P. Zhang, J.L. Zhang, S.F. Shao, Y.Q. Tan, C.L. Wang, *Appl. Phys. Lett.* 94 (2009) 032902.
- [8] W.F. Liu, X.B. Ren, *Phys. Rev. Lett.* 103 (2009) 257602.
- [9] Z. Yu, C. Ang, R.Y. Guo, A.S. Bhalla, *J. Appl. Phys.* 92 (2002) 1489.
- [10] Z.Y. Feng, X.B. Ren, *Appl. Phys. Lett.* 91 (2007) 032904.
- [11] Y. Hidaka, S. Tsukada, J. Kano, S. Kojima, *Proceedings of the 2007 16th IEEE International Symposium on Applications of Ferroelectrics*. (2007) 305.
- [12] L. Zhang, L. Ben, O.P. Thakur, A. Feteira, A.G. Mould, D.C. Sinclair, A.R. West, *J. Am. Ceram. Soc.* 91 (2008) 3101.
- [13] X.Q. Jin, Y.J. Luo, Y. Lu, L.L. Zhang, D.Z. Sun, *Ferroelectrics* 363 (2008) 163.
- [14] H.L. Du, F.S. Tang, F. Luo, W.C. Zhou, S.B. Qu, Z.B. Pei, *Mater. Sci. Eng. B* 137 (2007) 175.
- [15] J. Fu, R.Z. Zuo, Y. Liu, *J. Alloys Compd.* 493 (2010) 197.
- [16] E. Hollenstein, D. Damjanovic, N. Setter, *J. Eur. Ceram. Soc.* 27 (2007) 4093.
- [17] S.J. Zhang, R. Xia, T.R. Shrout, *Appl. Phys. Lett.* 91 (2007) 132913.
- [18] R.Z. Zuo, J. Fu, D.Y. Lv, *J. Am. Ceram. Soc.* 92 (2009) 283.
- [19] R.Z. Zuo, J. Fu, D.Y. Lv, Y. Liu, *J. Am. Ceram. Soc.* 93 (2010) 2783.
- [20] D. Hennings, H. Schnell, G. Simon, *J. Am. Ceram. Soc.* 65 (1982) 539.
- [21] X.G. Tang, K.H. Chew, J. Wang, H.L.W. Chan, *Appl. Phys. Lett.* 85 (2004) 991.
- [22] T. Maiti, R. Guo, A.S. Bhalla, *J. Am. Ceram. Soc.* 91 (2008) 1769.
- [23] J.L. Zhang, X.J. Zong, L. Wu, *Appl. Phys. Lett.* 95 (2009) 022909.
- [24] X. Wang, C.N. Xu, H. Yamada, K. Nishikubo, X.G. Zheng, *Adv. Mater.* 17 (2005) 1254.
- [25] L.L. Zhang, X.S. Wang, H. Liu, X. Yao, *J. Am. Ceram. Soc.* 93 (2010) 1049.
- [26] S.H. Park, C.W. Ahn, S. Nahm, J.S. Song, *Jpn. J. Appl. Phys.* 43 (2004) 1072.
- [27] A. Cohen, R.C. Bradt, G.S. Ansell, *J. Am. Ceram. Soc.* 53 (1970) 396.
- [28] H.Y. Chen, X.B. Guo, Z.Y. Meng, *Key Eng. Mater.* 224 (2002) 89.
- [29] J.H. Liao, S.Y. Cheng, C.H. Wang, *1990 IEEE 7th Int Symp Appl Ferroelectr.* (1992) 443.